Available online at www.sciencedirect.com

ScienceDirect

Ceramics International 40 (2014) 16829–16834

CERAMICS INTERNATIONAL

www.elsevier.com/locate/ceramint

Short communication

A comparative study of the pressureless sinterability of 3 mol% Y_2O_3-stabilized ZrO_2 powders prepared by the sol–gel method under different synthesis conditions without modifiers

Nadia Mamana[a], Angel L. Ortiz[b], Florentino Sánchez-Bajo[c], Ricardo Caruso[a,*]

[a]*Laboratorio de Materiales Cerámicos, Instituto de Física de Rosario (CONICET-UNR), Avda. 27 de febrero 210 Bis, 2000 Rosario, Argentina*
[b]*Departamento de Ingeniería Mecánica, Energética y de los Materiales, Universidad de Extremadura, Avda. de Elvas S/N, 06006 Badajoz, Spain*
[c]*Departamento de Física Aplicada, Universidad de Extremadura, Avda. de Elvas S/N, 06006 Badajoz, Spain*

Received 18 March 2014; received in revised form 30 July 2014; accepted 4 August 2014
Available online 12 August 2014

Abstract

A wide set of 3 mol% Y_2O_3-stabilized ZrO_2 (3YSZ) powders have been synthesized by the sol–gel method without modifiers from solutions of zirconium *n*-propoxide and yttrium acetate prepared with different water/Zr molar ratio and zirconium concentration, and the effect of these two synthesis variables on the pressureless sinterability of the 3YSZ powders has been investigated. It was found that the sinterability increases with increasing zirconium concentration and water/Zr molar ratio, which is attributed to the smaller cluster size developed during the sol–gel synthesis. Implications for the preparation of more sinterable 3YSZ powders are discussed.
© 2014 Elsevier Ltd and Techna Group S.r.l. All rights reserved.

Keywords: D. ZrO_2; Sol–gel; Powder; Microstructure; Densification

1. Introduction

ZrO_2-based ceramics are well known for their excellent set of mechanical, electronic, thermal, and optical properties [1,2]. Not surprisingly, Y_2O_3-stabilized ZrO_2 (and particularly those with 3 mol% doping Y_2O_3, or hereafter 3YSZ) ceramics with a dense, fine-grained microstructure are regarded as high-performance ceramic materials, and are therefore used in many structural applications. Several synthesis methods have been reported [3,4] for the preparation of 3YSZ powders with the appropriate sintering behavior required for the processing of dense, fine-grained 3YSZ bulk ceramics. Among them, the sol–gel method is often used in the synthesis of oxide ceramic powders, as the 3YSZ powders, because it provides a series of advantages in relation to other methods [5] such as for example that it is amenable to the production of high purity, reactive, and chemically homogeneous powders with excellent properties [5,6,7]. The sol–gel method is based on the hydrolysis and inorganic polymerization reactions of metal alkoxides. One can therefore understand that the nature and molar ratio of modifiers/Zr (the former being for example acetic acid, acetylacetone, etc.) are important synthesis variables that may affect the kinetics and therefore the evolution of the sol–gel reactions for the synthesis of ZrO_2-based powders. Other synthesis variables as for example the H_2O/Zr molar ratio and the zirconium concentration may also have great influence on the synthesis of ZrO_2-based powders. The appropriate control of these two synthesis variables is certainly important because they are expected to condition strongly the crystallization and morphological aspects of the resulting powders, and the powder features in turn condition the sintering behaviour. For this reason, several studies have reported the influence of variations in the H_2O/Zr molar ratio and zirconium concentration on the features of the products obtained from sol–gel solutions. However, most of these studies used modifiers of the synthesis [8,9,10].

Recently, we have reported the results of a sol–gel synthesis study of 3YSZ powders carried out in the absence of

*Corresponding author. Tel.: +54 341 4495467; fax: +54 341 4495467x37.
E-mail address: rcaruso@fceia.unr.edu.ar (R. Caruso).

http://dx.doi.org/10.1016/j.ceramint.2014.08.015
0272-8842/© 2014 Elsevier Ltd and Techna Group S.r.l. All rights reserved.

modifiers [11]. We were able to obtain powders with greater sinterability at 1200 °C, [11] although unfortunately the sintered compacts still had a large residual porosity (i.e., ~25%). With this in mind, this study was undertaken to take a step forward towards the obtaining of even more sinterable 3YSZ powders via the control of the sol–gel synthesis. To that end, here we have synthesized, and characterized, 3YSZ powders from the sol–gel solutions prepared under different H_2O/Zr molar ratio and zirconium concentration in the absence of synthesis modifiers, and have compared their degree of pressureless densification at 1200 °C with the broader objective of elucidating synthesis effects on the sinterability of 3YSZ powders. The present study is therefore focused exclusively on identifying chemistry effects on the sinterability of the 3YSZ powders, with the detailed investigation of their complete densification deferred to later reports.

2. Experimental

2.1. Solution and powder preparation

The starting solutions were prepared by stirring zirconium *n*-propoxide (ZNP; 70 wt% in *n*-propanol) and *n*-propanol (PrOH), in an anhydrous nitrogen atmosphere. The 3YSZ solutions were obtained by adding yttrium acetate (99.9% Aldrich) dissolved in propanol and nitric acid to the starting ZNP solutions.

Under magnetic stirring, different amounts of distilled water were carefully added to obtain 3YSZ solutions with different H_2O/Zr molar ratio, which hereafter will be referred to as *h* values. In particular, the H_2O/Zr molar ratio chosen were 2, 3, 4, 5, 6, 8, 10 and 12; accordingly, these solutions (S) were labeled as Sh2, Sh3, Sh4, Sh5, Sh6, Sh8, Sh10, and Sh12, respectively. The *n*-propanol volumes were adjusted to obtain a zirconium concentration of 0.66 M. In all cases, the formation of a white gel was observed within the first 10 min after the water addition.

Five starting solutions of 3YSZ were also prepared, where the zirconium concentration was conveniently varied, which hereafter will be referred to as Zr values, while the *h* value was fixed at 6. The zirconium concentration chosen were 0.2, 0.4, 0.66, 0.8, and 0.9 M, and therefore these solutions (S) were labeled as SZr02, SZr042, SZr066, SZr08, and SZr09, respectively. Once again, formation of a white gel occurred in the five cases within the first 10 min after the water addition.

Powders were subsequently obtained by drying the gels at 100 °C for 48 h in air, and were labelled as the parent solutions but using the letter P (powders) instead of S (solutions). The resulting powders were then heat-treated at temperatures in the range 100–1250 °C for 1 h in air atmosphere, to eliminate the residual products of the sol–gel synthesis. The elementary analysis of carbon was performed using a carbon analyzer (model LECO-200). Table 1 lists the nomenclature and composition of the different sol–gel solutions and 3YSZ powders prepared in this study.

Next, pellets were prepared by uniaxial pressing at 200 MPa of the powders previously heat-treated at 500 °C and then crushed with a mortar and pestle. Finally, the compacts were sintered at 1200 °C for 2 h in air atmosphere using a heating rate of 3 °C/min (ORL electric furnace). These particular sintering conditions were chosen for comparison purposes only within the confines of the present sinterability study, not with a view to fully densifying the 3YSZ powders.

The microstructure of selected sintered ceramics was examined by scanning electron microscopy (FE-SEM; Quanta 200F, FEI, The Netherlands), using conventional methods applicable to ceramic materials.

2.2. Characterization

Simultaneous differential thermal analysis/thermogravimetric analysis (DTA/TG; model DTG-60/60H, Shimadzu) studies were conducted using ~10 mg of the different powders. The measurements were carried out in air over the temperature range 25–1200 °C with heating and cooling rates of 10 °C/min, using α-Al_2O_3 as reference material.

X-ray diffraction (XRD) patterns were collected (model X'Pert Pro MDP) at room temperature. The XRD data were measured over the angular range $20-100^\circ 2\theta$ with a step size of 0.02° and a counting time of 1 s per step, using Cu*K*α incident radiation and 0.3074° instrumental broadening. The XRD patterns were then analyzed by the Rietveld method, using the FullProf software.

The residual porosity in the sintered compacts was measured by the Archimedes method in distilled water.

3. Results and discussion

3.1. Thermal analysis

Fig. 1 shows the elementary analysis of carbon for the powder labeled as Ph6 as a function of the heat-treatment temperature (100–1250 °C) in air for 1 h. Clearly, this type of curves informs on the dependence of the elimination of the organic residuals of the sol–gel synthesis with the heat-treatment. It can be seen in Fig. 1 that the complete elimination of organic residuals occurred between 400 and 500 °C, that is when the curve flattened. The powders collected after the heat-treatments were of gray color if calcined up to 400 °C and however of white color if calcined at or above 500 °C.

The shape of the curves carbon content vs. calcinations temperature for the rest of 3YSZ powders was similar to that of the powder Ph6, and therefore they will not be presented. Fig. 2 shows the DTA–TG analyses for the powder labeled as Ph6. It can be seen that there is an endothermic peak at ~75 °C, which is associated to the elimination of the physically-adsorbed water and solvent. In the temperature range 300–450 °C one can see a continuous mass loss in the TG curve, together with two exothermic peaks that are caused by the elimination of the bound water and organics [12,13]. At ~460 °C, an exothermic peak appeared in the DTA curve without mass loss in the TG curve, which has been reported as being due to the crystallization of the ZrO_2 [14]. Taken together, the elementary analysis of carbon and the DTA–TG analyses indicate that the crystallization of the

Table 1
Designation of the sol–gel solutions and powders, and their synthesis conditions.

Solution	H_2O/Zr	Zirconium concentration	Powder
SZr02	6	0.2	PZr02
SZr04	6	0.4	PZr04
SZr066	6	0.66	PZr066
SZr08	6	0.8	PZr08
SZr09	6	0.9	PZr09
Sh2	2	0.66	Ph2
Sh3	3	0.66	Ph3
Sh4	4	0.66	Ph4
Sh5	5	0.66	Ph5
Sh6	6	0.66	Ph6
Sh8	8	0.66	Ph8
Sh10	10	0.66	Ph10
Sh12	12	0.66	Ph12

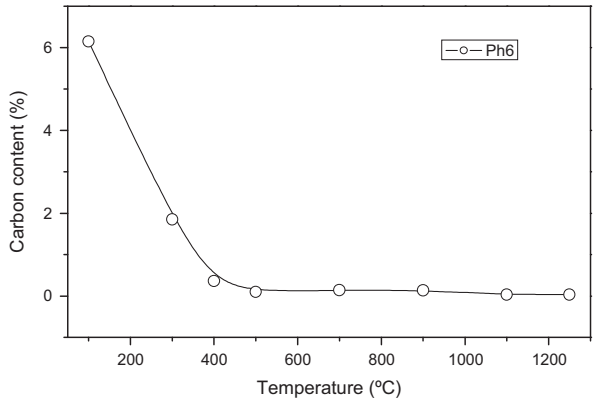

Fig. 1. Elementary analysis of carbon for the powder Ph6 as a function of the heat-treatment temperature in air for 1 h.

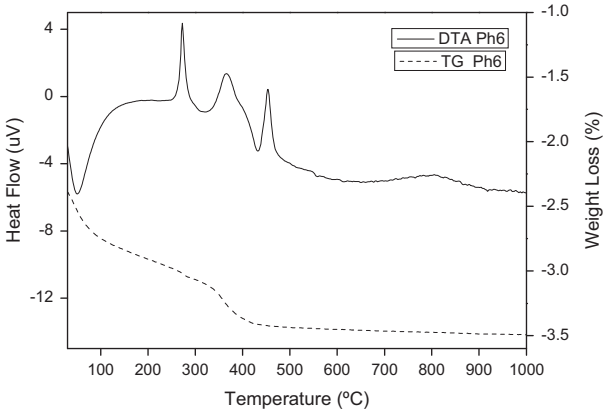

Fig. 2. DTA–TG curves up to 1000 °C in air for the powder Ph6.

3YSZ powders only occurs after the calcination-induced elimination of the residual of the sol–gel synthesis [15]. The general description of the DTA–TG curve made for Ph6 is also applicable to the rest of 3YSZ powders.

With this information, it is then reasonable to choose the 3YSZ powders calcined at 500 °C as being the most appropriate ones for the subsequent comparative sintering studies, and therefore they will next be characterized in more detail.

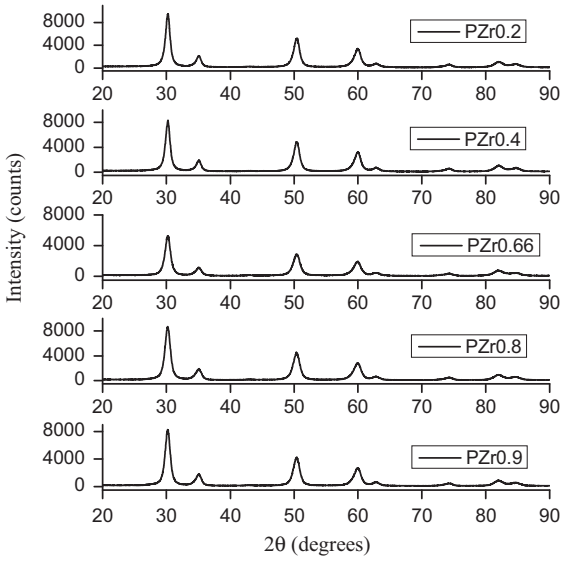

Fig. 3. XRD patterns of the 3YSZ powders prepared with different zirconium concentration and then calcined at 500 °C in air for 1 h.

3.2. XRD analysis

Figs. 3 and 4 show the XRD patterns of the 3YSZ powders calcined at 500 °C in air for 1 h that had been prepared using different zirconium concentration and H_2O/Zr molar ratio, respectively. Clearly, these XRD patterns rule out the monoclinic phase, and suggest the presence of tetragonal phase as major phase. Detailed Rietveld analyses of these XRD patterns, as the one shown in Fig. 5 for the powder labeled as Ph6, indeed indicated that the only phase present in all the 3YSZ powders is the tetragonal phase. The XRD patterns of the 3YSZ powders calcined at 1200 °C (not shown), which exhibited much less peak broadening, confirmed this conclusion by showing the peak doublet at $\sim 74^\circ 2\theta$ that is certainly characteristic of the tetragonal 3YSZ phase.

The Rietveld analyses also enabled the determination of the lattice parameters of the tetragonal 3YSZ structure (both a and c). The so-measured values are given in Table 2, together with the c/a ratio. In principle, according to the existing bibliography [16] the c/a ratio should be ~ 1.433. As can be seen in Table 2, this is indeed that value determined by the Rietveld analyses for the 3YSZ powders prepared with H_2O/Zr value equal or greater than 6, indicating an increase in the tetragonality of the crystalline structure [17,18]. However, the powders prepared with lower H_2O/Zr values exhibit a c/a ratio in the range $1.426-1.428$, due in general to their greater a values and lower c values. These c/a ratios are slightly lower that what is expected for the tetragonal 3YSZ phase (a=3.6099 Å and c=5.1738 Å), and in principle surprises because the c/a ratio should depend mainly on the doping composition and not on the conditions of the sol–gel synthesis.

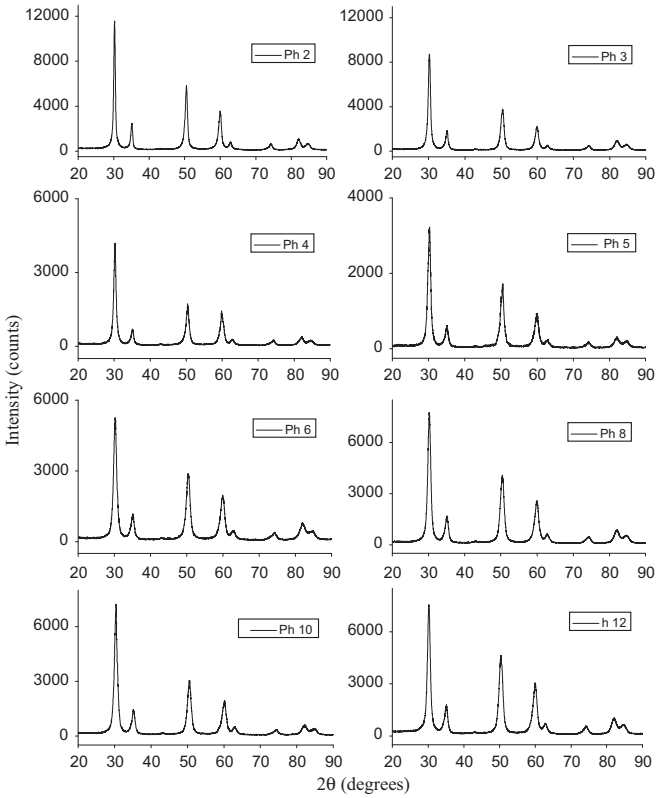

Fig. 4. XRD patterns of the 3YSZ powders prepared with different H_2O/Zr molar ratio and then calcined at 500 °C in air for 1 h.

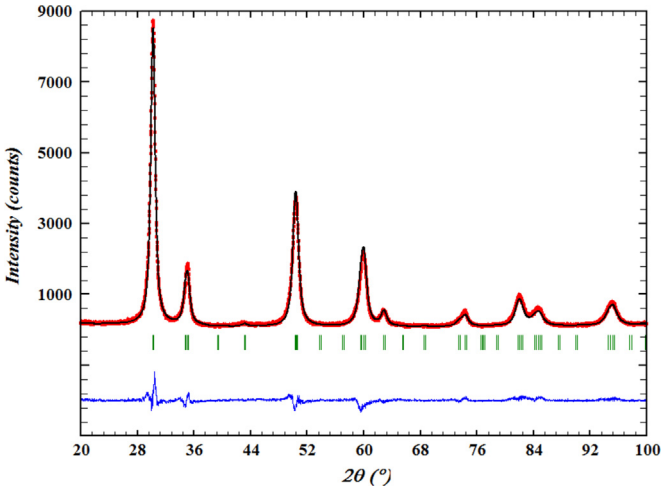

Fig. 5. Plotted output from the Rietveld analysis of the powder Ph6 calcined at 500 °C in air for 1 h. The dotted points are the experimental data, the solid red line is the Rietveld fit, and the solid blue line is the difference plot. The positions of YSZ Bragg reflections (calculated according to the Rietveld-fitted lattice parameters) are shown as green vertical bars. (For interpretation of the references to color in this figure legend, the reader is referred to the web version of this article.)

Also, it can be seen in Table 2 that except for the zirconium concentration with a value of 0.2, the rest of zirconium concentration values led to the expected *c/a* ratio for the 3YSZ structure.

Table 2
Lattice parameters determined by the Rietveld analysis of the XRD patterns of the different 3YSZ powders prepared by the sol–gel method and then calcined at 500 °C in air for 1 h.

Powder	*a* (Å)	*c* (Å)	*c/a*
PZr02	3.6081	5.1539	1.428
PZr04	3.6066	5.16	1.431
PZr066	3.6068	5.1647	1.432
PZr08	3.6073	5.1631	1.431
PZr09	3.6074	5.1596	1.430
Ph2	3.6094	5.1465	1.426
Ph3	3.6093	5.1544	1.428
Ph4	3.6095	5.1523	1.427
Ph5	3.5986	5.1414	1.429
Ph6	3.6067	5.164	1.432
Ph8	3.6068	5.1609	1.431
Ph10	3.6058	5.16	1.431
Ph12	3.5981	5.1577	1.433

3.3. Comparative densification study

Table 3 lists the residual porosity of the compacts sintered at 1200 °C in air for 2 h from the different 3YSZ powders synthesized here, and then calcined at 500 °C. Clearly, the porosity of the sintered body decreases markedly with increasing the zirconium concentration and H_2O/Zr molar ratio. In this latter case, the porosity decreases with increasing H_2O/Zr molar ratio concentration up to 12, above which no further reduction in porosity was observed (not shown).

Fig. 6 shows representative FE-SEM images of the microstructure of two selected ceramics sintered at 1200 °C for 2 h in air. A homogeneous grain size distribution is observed in both cases, with some residual porosity. It can also be seen that that the grain size of the Ph6 and Ph12 ceramics is similar and within the nanometer scale (~100 nm). Therefore, the porosity differences (see Table 3) between both ceramics (Ph6 and Ph12) are not induced by the grain size, but by a different sintering behaviour resulting from the use of a different H_2O/Zr molar ratio.

Also, the grain size does not seem to be affected by the heating ramp either. Thus, Fig. 7 shows a representative SEM image of the ceramic also resulting from the sintering of the Ph6 powder at 1200 °C for 2 h in air, but this time using a heating rate of 1 °C/min instead of 3 °C/min. Comparison with Fig. 6 indicates that the grain size (~100 nm) and the residual porosity(~25%) are not affected by this change in heating rate, from where it can be inferred that the powders have a good thermal stability.

Therefore, taken together, the trends in Table 3 and the FE-SEM examinations reveal that it is potentially possible to increase the pressureless sinterability of the 3YSZ powders, while obtaining nano or ultra-fine grained ceramics, by controlling the sol–gel synthesis conditions in the absence of modifiers. These conclusions, which are drawn from densification data obtained within the intermediate stage of sintering, are expected to remain valid once the sintering conditions have

been conveniently optimized to reach full dense 3YSZ ceramics.

To explain these observations it is necessary to consider in more depth the hydrolysis and condensation reactions occurring during the sol–gel synthesis. It is well known that due to the hydrolysis reaction an alkoxide group is hydrolyzed to form a group of ZrOH and alcohol, as follows: $Zr(OPr)_4 + nH_2O \rightarrow Zr(OH)_n(OPr)_{4-n} + n$PrOH. Then, by the condensation reaction two species with a metallic center (i.e., monomer) react originating a species with two metallic centers (i.e., dimer). If the condensation involves two hydrolyzed species of the type $(Zr(OH)n(OPr)_{4-n})$, then the reaction is named oxolation. However, if the reaction involves an hydrolysed species and an alkoxide group of the type $(Zr(OPr)_4)$, then the reaction is named alcoxolation. While the reaction continues, several metallic centers are joined together forming clusters that continue to grow according to the mechanism of monomer-cluster growth. Consequently, the 3YSZ solutions prepared with higher H_2O/Zr molar ratio have lesser number of metallic centers (monomers) in solution, and will therefore be more prone to form smaller clusters or, in other words, smaller powder particles with greater surface area for otherwise identical sol–gel synthesis conditions. This provides these 3YSZ powders with greater reactivity during pressureless sintering, and the improved sinterability results in denser compacts under the same sintering conditions. It is thus acknowledged that specific surface area, sizes of cluster, crystallite and particle, and other powder features have to be investigated in more detail, which nonetheless deferred for future work. Furthermore, in the case of the 3YSZ powders prepared with different H_2O/Zr values, it seems that the degree of densification also increases with increasing the *c*/*a* ratio of the tetragonal 3YSZ structure, most likely due to that the greater crystallographic distortion results in an increase of free energy and decrease in bonding energy, and therefore in greater atom diffusivity.

Table 3
Degree of residual porosity (%) in the compacts sintered at 1200 °C in air for 2 h from 3YSZ powders prepared using different zirconium concentration and H_2O/Zr molar ratio.

Sample	Porosity (%)
PZr02	31
PZr04	28
PZr066	25
PZr08	21
PZr09	21
Ph2	45
Ph3	37
Ph4	32
Ph5	27
Ph6	25
Ph8	21
Ph10	19
Ph12	19

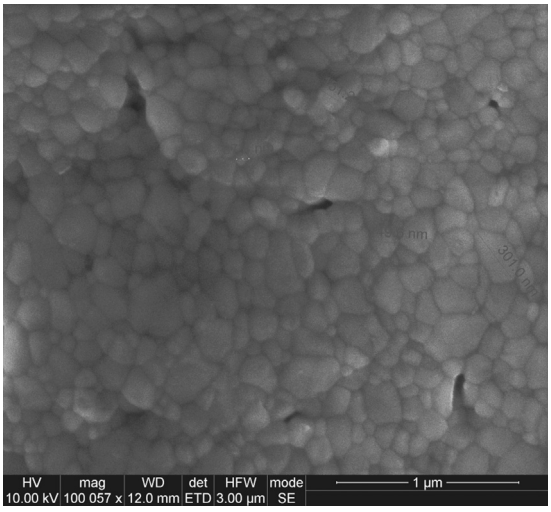

Fig. 7. SEM micrographs of the 3YSZ ceramics obtained by pressureless sintering at 1200 °C for 2 h in air with a heating rate of 1 °C/min from the powders Ph6.

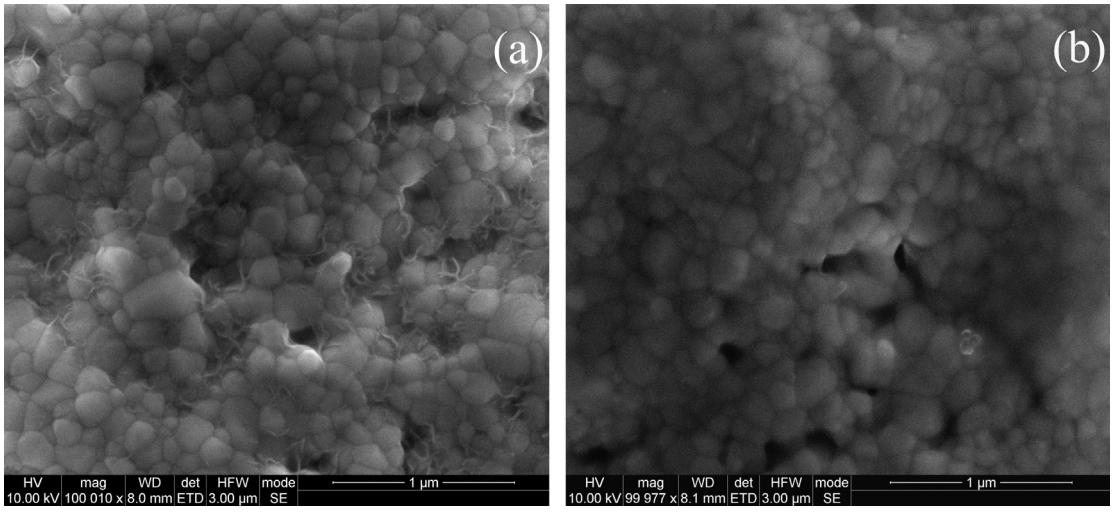

Fig. 6. SEM micrographs of the 3YSZ ceramics obtained by pressureless sintering at 1200 °C for 2 h in air with a heating rate of 3 °C/min from the powders: (a) Ph6, and (b) Ph12.

4. Conclusions

We have investigated the effect of the zirconium concentration and H_2O/Zr molar ratio chosen during the modifier-free preparation of 3YSZ sol–gel solutions on the pressureless sinterability of the resulting powders. Based on the results and analyses, the following conclusions can be drawn:

1. Crystallization of the 3YSZ phase occurs once the organic residual from the sol–gel synthesis have been eliminated, and takes place in its tetragonal structure.
2. Sol–gel synthesis variables such as the zirconium concentration and H_2O/Zr molar ratio in the absence of modifiers affect the features of the resulting 3YSZ powders.
3. 3YSZ powders obtained from sol–gel solutions with higher zirconium concentration and/or H_2O/Zr molar ratio have greater pressureless sinterability, which is most likely due to the smaller cluster size developed during the sol–gel synthesis.
4. A doping content of only 3 mol% Y_2O_3 during the sol–gel synthesis is sufficient to stabilize the ZrO_2 tetragonal phase during the heating and cooling cycles, at least between room temperature and 1200 °C.

References

[1] N.Q. Minh, Ceramic fuel cells, J. Am. Ceram. Soc. 76 (3) (1993) 563–589.

[2] Y. Miyahara, K. Tsukada, H. Miyagi, Field-effect transistor using a solid electrolyte as a new oxygen sensor, J. Appl. Phys 63 (1988) 2431.

[3] Y. Gu, G. Li, G. Meng, D. Peng, Sintering and electrical properties of coprecipitation prepared $Ce_{0.8}Y_{0.2}O_{1.9}$ ceramics, Mater. Res. Bull. 35 (2000) 297.

[4] G. Dell'Agli, G. Mascolo, Hydrothermal synthesis of ZrO_2–Y_2O_3 solid solutions at low temperature, J. Eur. Ceram. Soc. 20 (2) (2000) 139–145.

[5] C.W. Kuo, Y.H. Lee, K.Z. Fung, M.C. Wang, Effect of Y_2O_3 addition on the phase transition and growth of YSZ nanocrystallites prepared by a sol–gel process, J. Non-Cryst. Solids 351 (4) (2005) 304–311.

[6] M.Z. C. Hu, R.D. Hunt, E.A. Payzant, C.R. Hubbard, Nanocrystallization and phase transformation in monodispersed ultrafine zirconia particles from various homogeneous precipitation methods, J. Am. Ceram. Soc. 82 (1999) 2313–2320.

[7] M.Z. C. Hu, V. Kurian, E.A. Payzant, C.J. Rawn, R.H. Hunt, Wet chemical synthesis of monodispersed barium titanate particles—hydrothermal conversion of TiO_2 microspheres to nanocrystalline $BaTiO_3$, J. Powder Technol. 110 (2000) 2–14.

[8] C. Viazzi, A. Deboni, J. Ferreira, J. Bonino, F. Ansart, Synthesis of yttria stabilized zirconia by sol–gel route: influence of experimental parameters and large scale production, Solid State Sci. 8 (2006) 1023–1028.

[9] H. Hayashi, H. Susuki, S. Kaneko, Effect of the chemicals modification on hydrolysis and condensation reaction of zirconium alkoxide, J. Sol–gel Sci. Technol. 12 (1998) 87–94.

[10] X. Changrong, C. Huaqiang, W. Hong, Y. Pinghua, M Guangyao, P. Dingkun, Sol–gel synthesis of yttria stabilized zirconia membranes through controlled hydrolysis of zirconium alcoxide, J. Membr. Sci. 162 (1999) 181–188.

[11] N. Mamana, A. Díaz-Parralejo, A.L. Ortiz, F. Sánchez-Bajo, R. Caruso, Influence of the synthesis process on the features of Y_2O_3-stabilized ZrO_2 powders obtained by the sol–gel method, Ceram. Int. 40 (2014) 6421–6426.

[12] R. Caruso, N. Pellegri, O. de Sanctis, M.C. Caracoche, P. Rivas, ZrO_2 phase structure in coating films and powders obtained by sol gel process, J. Sol–Gel Sci. Technol. 3 (3) (1994) 241.

[13] P.C. Rivas, J.A. Martinez, M.C. Caracoche, A.R. Lopéz Garcia, Pertubed-angular-correlation study of zirconias produced by sol–gel method, J. Am. Ceram. Soc. 78 (5) (1995) 1329–1334.

[14] R. Caruso, O. de Sanctis, A. Macías-García, E. Benavidez, S.R. Mintzer, Influence of pH value and solvent utilized in the sol–gel synthesis on properties of derived ZrO_2 powders, J. Mater. Proc. Technol. 152 (2004) 299–303.

[15] M. Yashima, T.A. Kato, M. Kakihana, M.A. Gülgün, Y. Matsuo, M. Yoshimura, Crystallization of hafnia and zirconia during the pyrolysis of acetate gels, J. Mater. Res. 12 (1997) 2575–2583.

[16] H. Toraya, Effect of $YO_{1.5}$ dopant on unit-cell parameters of ZrO_2 at low contents of $YO_{1.5}$, J. Am. Ceram. Soc. 72 (4) (1989) 662–664.

[17] J. Luo, R. Stevens, Tetragonality of nanosized 3Y-TZP powders, J. Am. Ceram. Soc. 82 (7) (1999) 1922–1924.

[18] K. Yasuda, Y. Goto, H. Takeda, Influence of tetragonality on tetragonal-to-monoclinic phase transformation during hydrothermal aging in plasma-sprayed yttria-stabilized zirconia coatings, J. Am. Ceram. Soc. 84 (Issue 5) (2001) 1037–1042.